

## Supplementary Information for

### **High-resolution solid-state oxygen-17 NMR of actinide-bearing compounds: an insight into the 5*f*-chemistry**

Laura Martel<sup>\*1</sup>, Nicola Magnani<sup>1</sup>, Jean-Francois Vigier<sup>1</sup>, Jacobus Boshoven<sup>1</sup>, Chris Selfslag<sup>1</sup>,  
Ian Farnan<sup>2</sup>, Jean-Christophe Griveau<sup>1</sup>, Joseph Somers<sup>1</sup>, Thomas Fanghänel<sup>1</sup>

<sup>1</sup>European Commission, Joint Research Centre, Institute for Transuranium Elements,  
Hermann-von-Helmoltz-Platz 1, D-76344 Eggenstein-Leopoldshafen, Germany

<sup>2</sup>Department of Earth Sciences, University of Cambridge, Downing Street, Cambridge, CB2  
3EQ, UK.

<sup>\*</sup>[laura.martel@ec.europa.eu](mailto:laura.martel@ec.europa.eu)

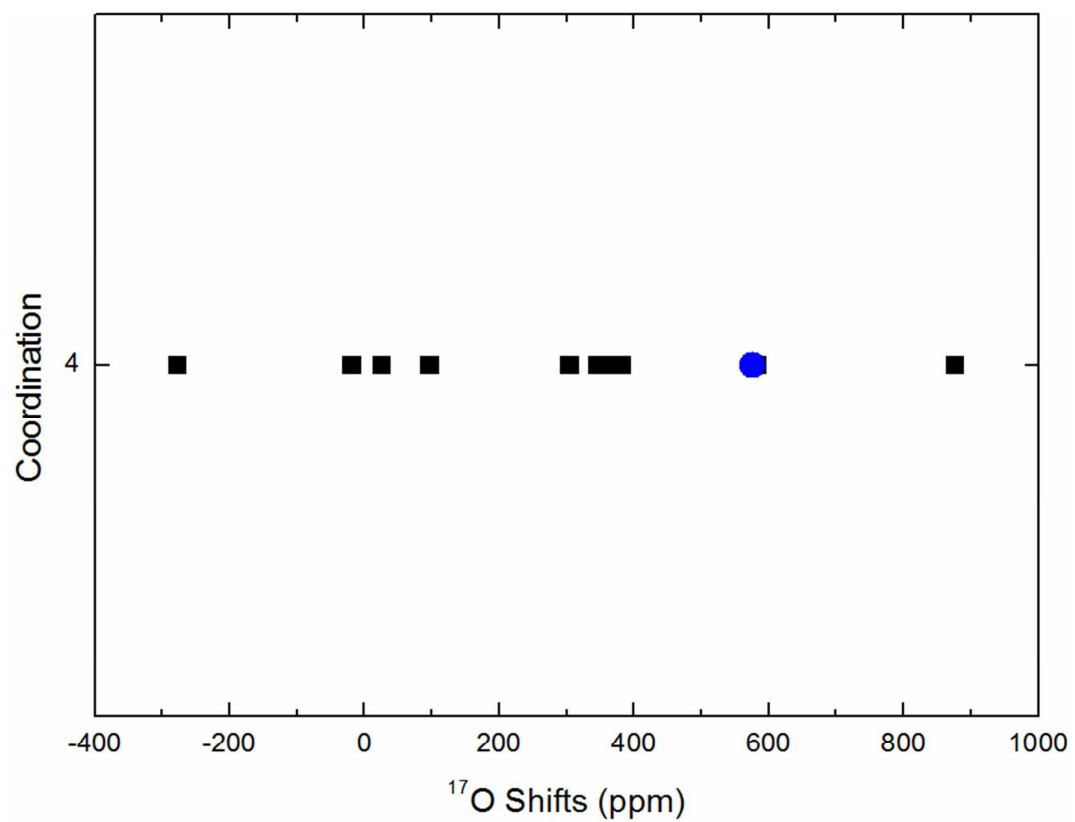


Figure S1:  $^{17}\text{O}$  shifts of diamagnetic metal oxides<sup>1</sup> (black squares) compared with that of  $\text{ThO}_2$  (blue circle).

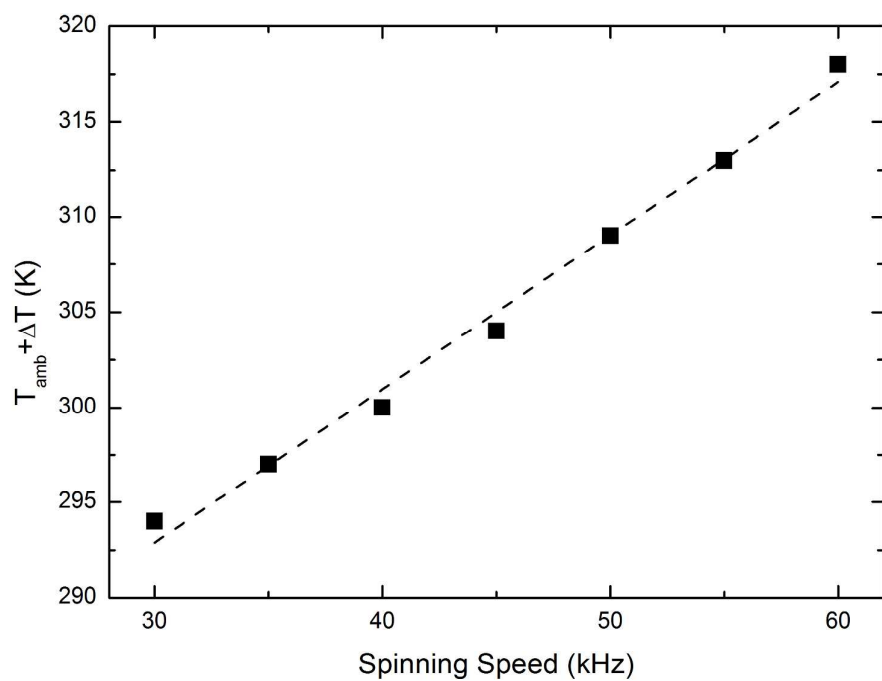


Figure S2: Evolution of the temperature (room temperature ( $T_{\text{amb}}$ ) with a gradient of temperature ( $\Delta T$ )) with increasing spinning speed. The temperatures have been determined using  $\text{Pb}(\text{NO}_3)_2$  correlations<sup>2</sup> The dashed line is a linear fit.

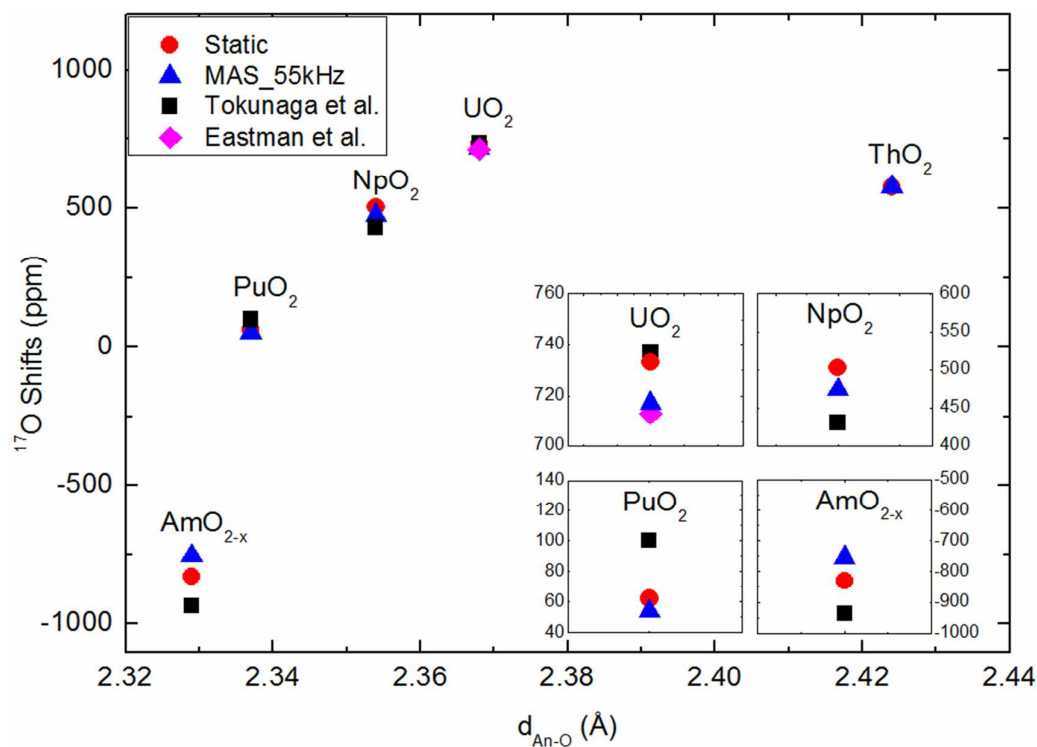


Figure S3: Evolution of the  $^{17}\text{O}$  shift as a function of the An-O distance. The results obtained in this study (static and MAS at 55 kHz) are compared with the previous static experiments published by Tokunaga et al.<sup>3</sup> (black squares) and Eastman et al. (pink diamond)<sup>4</sup>. The insets give a better view to compare the  $^{17}\text{O}$  shifts of each sample obtained in this study and by the other authors.

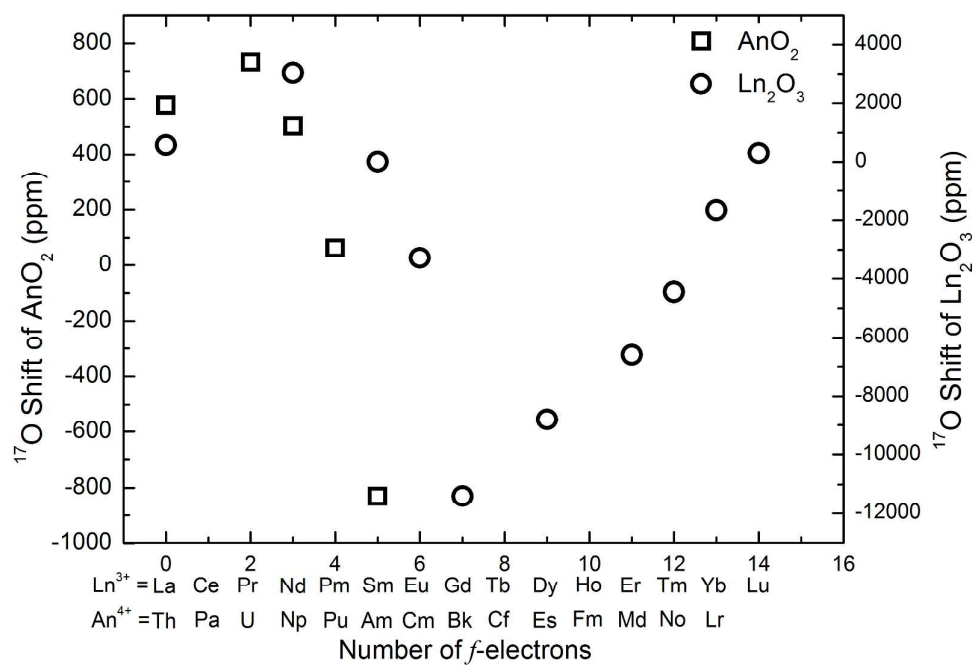


Figure S4: Evolution of the  $^{17}\text{O}$  chemical shifts in lanthanide ( $\text{Ln}_2\text{O}_3$ ) (from reference 5) and actinides ( $\text{AnO}_2$ ) dioxides as a function of the number of *f*-electrons.

Table S1:  $B_4$  and  $B_6$  are the crystal field (CF) parameters which appear in  $H_{CF}$  (see Equation 4 in main text), and are taken from the given literature references.  $A\langle S_z \rangle$  is calculated in several different ways to show the relevant trends: RS = Russell-Saunders coupling, no CF (i.e. only the lowest pure  $^{2S+1}L_J$  manifold is accounted for without removing its zero-field degeneracy); IC = Intermediate coupling, no CF (i.e.  $H_{FI}$  is diagonalized in order to take into account the mixing of excited  $^{2S+1}L'_J$  manifolds into the ground one, which remains  $2J+1$ -fold degenerate in zero field); RS+CF =  $H_{CF}$  is diagonalized within the lowest pure  $^{2S+1}L_J$  manifold, and  $A\langle S_z \rangle$  is calculated as a thermal average over the so-obtained wavevectors; IC+CF =  $H_{FI} + H_{CF}$  is diagonalized over the whole  $5f^n$  configuration states, and  $A\langle S_z \rangle$  is calculated as a thermal average over the so-obtained wavevectors. The results of the latter computational scheme are those presented in Figure 5.

Name	$B_4$ ( $\text{cm}^{-1}$ )	$B_6$ ( $\text{cm}^{-1}$ )	$A\langle S_z \rangle$ (RS)	$A\langle S_z \rangle$ (RS+CF)	$A\langle S_z \rangle$ (IC)	$A\langle S_z \rangle$ (IC+CF)
ThO <sub>2</sub>			0	0	0	0
UO <sub>2</sub>	-7950	3400	-3.20	-2.90	-2.24	-2.12
NpO <sub>2</sub>	-8500	3400	-4.91	-4.42	-3.13	-2.97
PuO <sub>2</sub>	-9750	4000	-4.80	-4.59	-1.12	-1.46
AmO <sub>2</sub>	-2200	–	-1.79	-1.97	-1.70	-0.14

## References

---

- 1 K. J. D. Mackenzie and M. E. Smith, Multinuclear Solid-State NMR of Inorganic Materials, *Pergamon Materials Series*.
2. Bielecki, A.; Burum, D.P. *J. Magn. Reson. A*, **116**, 215–220 (1995).
3. Tokunaga, Y., et al. NMR studies of actinide dioxides. *J. Alloys Compd.*, **444–445**, 241–245 (2007).
4. Eastman, M. P.; Hecht, H. G.; Lewis, W. B. *J. Chem. Phys.* **54**, 4141-4146 (1971).
5. Yang, S.; Shore, J.; Oldfield, E. *J. Magn. Reson.*, **99**, 408-412 (1992).